DTU Library

Geometric properties of optimal photonic crystals

Sigmund, Ole; Hougaard, Kristian G.

Link back to DTU Orbit

Geometric Properties of Optimal Photonic Crystals

Ole Sigmund* and Kristian Hougaard

*Department of Mechanical Engineering, Solid Mechanics, Technical University of Denmar Niels Koppels Allé, B. 404,
DK-2800 Lyngby, Denmark*

Photonic crystals can be designed to control and confine light. Since the introduction of the concept by Yablonovitch and John two decades ago, there has been a quest for the optimal structure, i.e., the periodic arrangement of dielectric and air that maximizes the photonic band gap. Based on numerical optimization studies, we have discovered some surprisingly simple geometric properties of optimal planar band gap structures. We conjecture that optimal structures for gaps between bands n and $n + 1$ correspond to n elliptic rods with centers defined by the generators of an optimal centroidal Voronoi tessellation (transverse magnetic polarization) and to the walls of this tessellation (transverse electric polarization).

PACS numbers: 42.70.Qs, 02.60.Pn

Photonic crystals (PhCs) are structures composed of periodic distributions of high and low index materials. With lattice constants of the order of the wavelength of light, PhCs can alter or inhibit its propagation [1,2]. PhCs are also called photonic band gap (PBG) structures, referring to the forbidden frequency bands where light cannot propagate through them. In order to control wide banded signals, it is of interest to find structures that have maximum relative band gap sizes. The gap center frequency can afterwards be controlled by simple geometric scaling. Depending on polarization, it seems to be well established that planar band gap structures for transverse magnetic (TM) polarization consist of triangular arrangements of circular high index (glass) rods in air and that structures for transverse electric (TE) polarization consist of triangular arrangements of circular low index (air) inclusions in a glass lattice. It is now well understood that the rod-based TM gaps can be explained by hopping (tunneling) between individual Mie resonators and that the hole-based TE gaps can be explained as a Bragg-like multiple scattering phenomenon [3]. However, optimality of these structures has not been proven, although it has been argued that they should be good due to the near circular shape of the associated Brillouin zone [4]. In general, their use is motivated by geometric simplicity, manufacturability, and extensive parametric studies [5]. In the quest for optimal planar band gap structures, a multitude of papers have reported parameter variation studies on various simple triangular, square, and hexagonal unit cell and inclusion shapes in lower and higher bands. However, few papers have considered the inverse problem: find the distribution of dielectric material in air (or opposite) that maximizes the relative band gap size. Previous inverse approaches can be divided into gradient-based approaches [6–8], exhaustive search methods [9], and evolutionary methods [10,11]. These papers have produced many interesting optimized topologies. However, clear conclusions about global optima are still missing.

In this Letter we conjecture that optimal PBG structures can be determined from simple geometric considerations. More specifically, we propose a simple geometric scheme that provides (near) optimal structures with gaps between any two bands. Based on our findings, we conjecture that the globally optimal structure for TM polarization *is* the triangular distribution of circular rods and that the globally optimal structure for TE polarization is a triangular distribution of hexagonal (instead of the commonly used circular) holes, i.e., the honeycomb structure. Our findings are based on the interpretation of an extensive numerical optimization study.

For lossless electromagnetic waves propagating in the xy plane, TM (**E** field in the z direction) and TE (**H** field in the z direction) polarized waves can be described by two decoupled wave equations

$$\nabla^2 E_z(\boldsymbol{x}) + \frac{\omega^2 \epsilon_r(\boldsymbol{x})}{c^2} E_z(\boldsymbol{x}) = 0, \qquad \text{TM}, \qquad (1)$$

$$\boldsymbol{\nabla} \cdot \left(\frac{1}{\epsilon_r(\boldsymbol{x})} \boldsymbol{\nabla} H_s(\boldsymbol{x}) \right) + \frac{\omega^2}{c^2} H_z(\boldsymbol{x}) = 0, \qquad \text{TE}. \qquad (2)$$

The distribution of dielectric is assumed periodic in the xy plane and constant in the z direction, i.e., $\epsilon_r(\boldsymbol{x} + \boldsymbol{R}_j) = \epsilon_r(\boldsymbol{x})$, where $\boldsymbol{R}_j$ are primitive lattice vectors with zero z component. The scalar fields satisfy the Floquet-Bloch wave conditions $E_z = e^{i\boldsymbol{k}\cdot\boldsymbol{x}} E_{\boldsymbol{k}}$ and $H_z = e^{i\boldsymbol{k}\cdot\boldsymbol{x}} H_{\boldsymbol{k}}$, respectively, where $E_{\boldsymbol{k}}$ and $H_{\boldsymbol{k}}$ are cell periodic fields. Solving (1) for wave numbers $\boldsymbol{k}$ belonging to the boundaries of the irreducible Brillouin zone we get a band diagram as shown in Fig. 1. We measure the relative band gap between bands n and $n + 1$ as

$$\frac{\Delta \omega_n}{\omega_n^0} = 2 \frac{\min_{\boldsymbol{k}}: \omega_{n+1}(\boldsymbol{k}) - \max_{\boldsymbol{k}}: \omega_n(\boldsymbol{k})}{\min_{\boldsymbol{k}}: \omega_{n+1}(\boldsymbol{k}) + \max_{\boldsymbol{k}}: \omega_n}(\boldsymbol{k}), \qquad (3)$$

where $\boldsymbol{k}$ are all wave vector values on the boundaries of the irreducible Brillouin zone. If $\Delta \omega_n / \omega_n^0 > 0$ for a particular
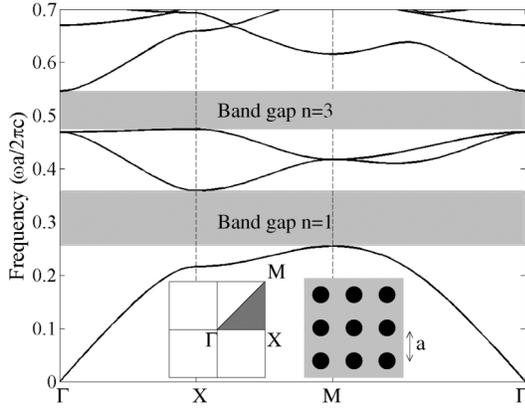
FIG. 1. Band diagram for a periodic arrangement of circular dielectric cylinders with $\epsilon_r = 11.56$ and radius $r/a = 0.25$ in air. The gray rectangles indicate band gaps where TM-polarized waves cannot propagate. Insets show the reciprocal lattice with the irreducible Brillouin zone indicated by the gray triangle (left) and the periodic lattice (right) with lattice constant a.

n, we say that there is a complete band gap between bands n and $n + 1$.

The open question is, what is the periodic distribution of dielectric $\epsilon_r(x + R_j) = \epsilon_r(x)$ that maximizes the relative band gap between any bands $\Delta\omega_n/\omega_n^0$? And further, what is the geometry that has the maximum band gap among all bands?

Our answer to the first question is the following: optimal band gap structures for gaps between bands n and $n + 1$ can be constructed geometrically by finding the minimum-energy distribution of n points in the unit cell that satisfy symmetry and periodicity requirements. The n points define the centers of n dielectric disks that make up the (near) optimal TM structure. Furthermore, a Voronoi tessellation [12] based on the n points gives a partition of the unit cell into n subdomains whose walls make up the (near) optimal TE structure.

The geometries described above are known as centrodial Voronoi tessellations and may be found as follows [12]: (1) Distribute n points in the unit cell satisfying symmetry and periodicity requirements. (2) Find the energy minimizing point distribution by the so-called Lloyd's algorithm, i.e., repeat (a) compute the Voronoi diagram corresponding to the point distribution, (b) compute the centroid of each cell of the Voronoi diagram, and (c) move each point to the centroid of the cell (still satisfying symmetry and periodicity requirements). (3) After convergence of Lloyd's algorithm, define the TM geometry as dielectric disks centered in the converged points and with radius $r/a \approx 0.40(\epsilon_r^d)^{-0.31}/\sqrt{n}$ (exponent based on numerical experiments) and define the TE geometry as the walls of the corresponding Voronoi diagrams with wall thickness $t/a \approx 0.40(\epsilon_r^d)^{-0.34}/\sqrt{n}$ where ϵ_r^d is the relative permittivity of the dielectric. The procedure is illustrated for the square unit cell, $n = 10$, and imposed 45° symmetry in Fig. 2. Optimal point positions and corresponding Voronoi
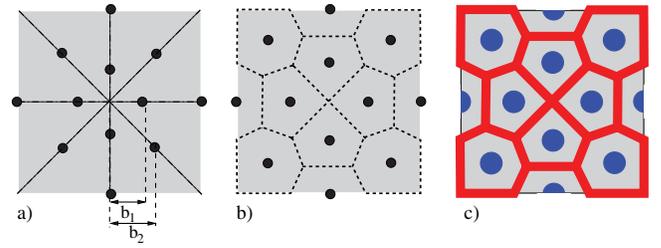

FIG. 2 (color). Geometrical procedure for generating (near) optimal planar band gap structures demonstrated on a square cell for band $n = 10$. (a) Initial point positions satisfying symmetry and periodicity for Lloyd's algorithm with free geometric parameters b_1 and b_2. (b) Converged point positions and associated Voronoi tessellation. (c) (Near) optimal TM structure (blue), TE structure (red), in air (gray).

tessellations for $n = 1$ to 15 computed for square and rhombic unit cells with imposed 45° and 30° symmetries are shown as black dots and dashed lines, respectively, in the composite Fig. 3. To answer the second question above, the global minimizer for Lloyd's algorithm is the regular hexagonal cell structure corresponding to a triangular distribution of generator points [12]. Hence, based on our findings, the globally optimal configuration for the TM case corresponds to a triangular arrangement of disk,s and for the TE case it is the perfect honeycomb structure.

In the following, we describe the numerical algorithm that leads to the above answers. The goal is to find the periodic and symmetric distribution of dielectric that maximizes the relative band gap (3) for either polarization case. The unit cell is discretized into $N \times N$ square or rhombic elements. The distribution of dielectric is determined in a pixel-like fashion by the pseudodensity vector $\boldsymbol{\rho}$ of length N^2, where the individual elements of $\boldsymbol{\rho}$ can take the value 0 (corresponding to air) or 1 (corresponding to dielectric). Hence, the spatial dielectric distribution can be described by $\epsilon_r(\boldsymbol{\rho}) = 1 + \boldsymbol{\rho}(\epsilon_r^d - 1)$, $\boldsymbol{\rho} \in (0, 1)^{N^2}$, where the relative permittivity of air is assumed to be unity. Based on this discretization and geometry description, we use the finite element method to solve (1) or (2) for the 16 lowest eigenvalues and 30 wave vector values evenly distributed along the boundaries of the irreducible Brillouin zone (Fig. 1). Relative band gap sizes are then found from (3).

Because of the complicated nature of the solution space, the optimization problem cannot be solved directly by gradient-based methods. On the other hand, evolution based or other random search algorithms will be inefficient due to the large number of design variables [$N^2 = O(10^4)$] needed to describe the geometry sufficiently accurately. Therefore, we start by an exhaustive search on coarse grids [Figs. 4(a) and 4(b)]. During the search, we store the 20 best topologies for each band. After a visual inspection, we select the 5 best topologically different candidates for each band and map the topologies to fine grids. Using the refined topologies as initial guesses, we use a gradient-based al-
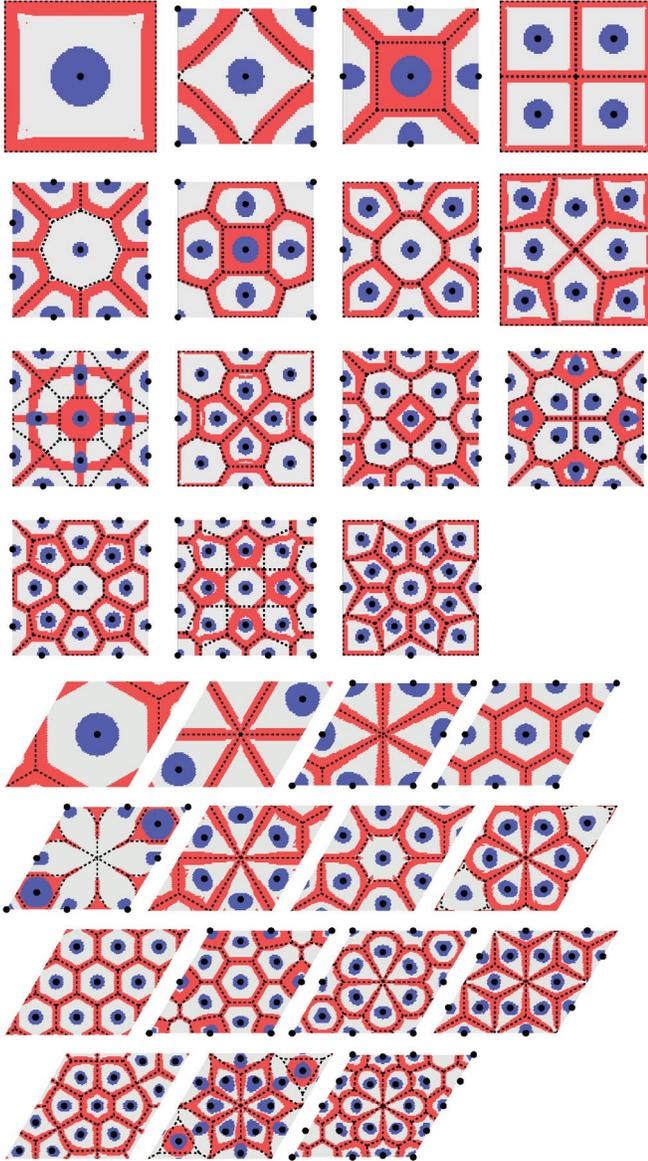
FIG. 3 (color). Composite picture showing optimal point positions (black dots) obtained from Lloyd's algorithm and corresponding Voronoi tessellations (dashed lines) for band numbers increasing from $n = 1$ (upper left) to $n = 15$ (lower right). Top: square unit cell; bottom: rhombic unit cell. Colors indicate topology optimized material distributions. Blue is the optimal distribution of dielectric for TM polarization, red is the optimal distribution for TE polarization, and gray indicates air.

gorithm known as topology optimization [6,7,13] to find the optimal fine grid structures [Fig. 4(c)].

The results of our optimization procedure applied to square and rhombic unit cells and $\epsilon_r^d = 11.56$ (corresponding to GaAs) are shown in Fig. 3. The composite plot shows the optimized TM structures for each band n in blue and the optimized TE structures in red. Gray indicates air. The results are surprisingly simple and visually pleasing. We observe that the optimized TM structures consist of evenly distributed elliptic or circular disks and that the optimized TE structures are subpartitioning closed-walled structures.
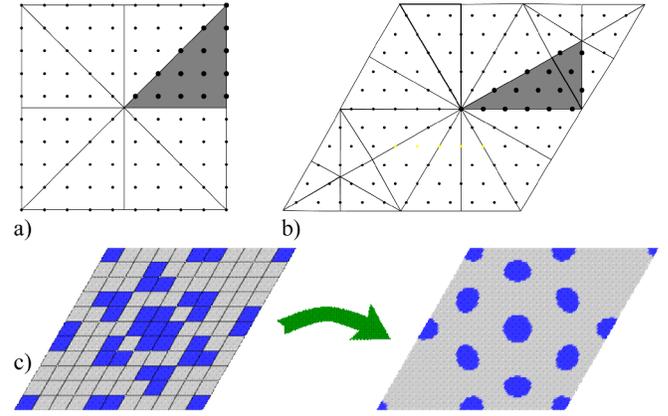

FIG. 4 (color online). Two-step optimization process. (a) Coarse grid with symmetry lines for (a) square unit cell with $N = 10$ and 15 free design variables, and (b) rhombic unit cell with $N = 11$ and 16 design variables. (c) Result of optimization process for coarse rhombic grid for band number $n = 10$ (left) and fine grid ($N = 89$) solution (right).

The number of disks and the number of subpartitions equal the band number n, and the TE structures seem to be Voronoi diagrams based on a point set defined by the centers of the TM disks. These observations lead us to the conclusions that optimal band gap structures can be constructed by simple geometric rules. It is also seen that the point positions (black dots) obtained from Lloyd's algorithm are virtually identical to the centers of the (blue) dielectric rods obtained from the topology optimization procedure for all bands, both square and rhombic unit cells. Also, in most cases the walls of the geometrically obtained Voronoi tessellations coincide with the topology optimized (red) dielectric distributions. One noteworthy exception is the optimal topology obtained for the square cell, band $n = 9$, where the topology optimized TE and TM structures correspond to two different local minima of Lloyd's algorithm. This indicates that, apart from the simple geometric properties of optimal band gap structures, the exact distribution of dielectric still plays a role in the determination of the optimal topologies and gap sizes—this explains our use of the term (*near*) optimal in describing the geometrically obtained structures. Modifications to the ideal geometries are also seen as ellipticity of the TM disks in the cases where the distances to nearest neighbors are varying (the long axis is oriented in the direction of the smaller neighbor distance; see, e.g., square cell gap $n = 3$ in Fig. 3). This is also observed for square cell gap $n = 5$, where the distance from the center point to all neighbors is large, resulting in a small diameter of the center disk.

To further support our conclusions, we compare the geometric energy of the centroidal Voronoi tessellations with the relative band gap sizes obtained by the topology optimization algorithm. The energy is defined as $\sum_{i=1}^{n} \int_{V_i} ||\mathbf{x} - \mathbf{x}_i|| d\mathbf{x}$, where V_i is the area of each Voronoi region and $\mathbf{x}_i$ is the coordinate of generating point
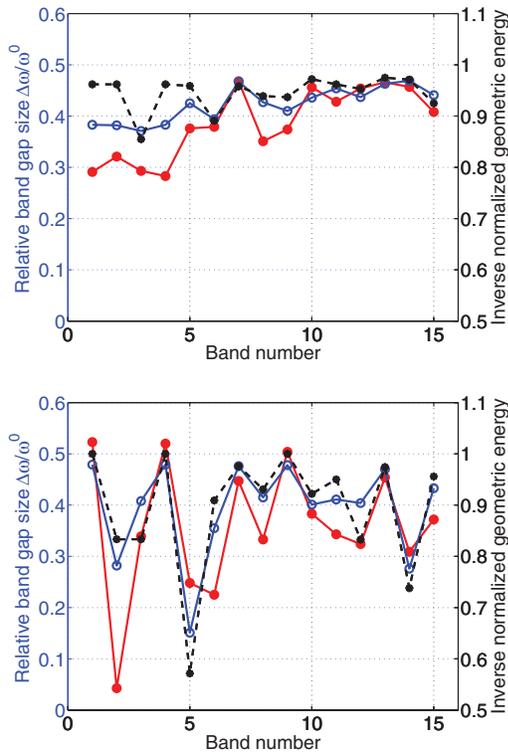
FIG. 5 (color).   Relative band gaps and geometric energies vs band number for square cell (top) and rhombic cell (bottom). Band gaps for TM polarization (blue lines and empty circles), TE polarization (red lines and filled circles), and inverse normalized energy (black dashed lines and stars).

i. If we take the inverse of this energy and multiply it with the energy of the perfect honeycomb, we get an inverse normalized energy that is unity for the optimal hexagonal partition and decreases for higher energy partitions. Energies and relative band gap sizes for the topology optimized structures are plotted with respect to the band number in Fig. 5. The correlation is seen to be very good. Gap size variations with respect to band number are much smaller for the square cell since energy and band gap minimizing hexagonal partitions do not fit into the square unit cell for small *n* with the imposed symmetry. On the other hand, the rhombic unit cell allows for both the optimal hexagonal cell partition (bands $n = 1$, 4, and 9) and the worst case partitions (bands $n = 2$ and 5), hence providing much bigger variations in gap sizes. The maximum relative band gap size over all bands and unit cell geometries and TM polarization is 0.48 for the triangular distributions of circular disks in the rhombic unit cells (for bands 1, 4, and 9) and 0.52 for TE polarization with the honeycomblike structures with hexagonal air inclusions in the rhombic unit cells (for bands 1, 4, and 9).

Our results provide a new understanding of previous findings from the literature. The optimal triangular pattern of rods for the TM case maximizes the distance between individual rods and hence retards tunneling between Mie resonators, and the corresponding TE structures are the best possible realization of an isotropic equidistance 2D Bragg grating. Also, most of our optimized square cell structures can be found in Ref. [8]. For those cases where there are discrepancies, our band gap sizes are larger. In [11] it is suggested that relaxation of symmetry requirements may increase gap size. This is true, and we note that their optimized structure is the best possible realization of a hexagonal hole structure in a square cell. Again, this confirms our conclusions.

The optimality of triangular arrangements of disks for the TM case is already generally accepted. For the TE case, the triangular arrangement of circular holes is the established geometry; however, the gain in relative band gap size is probably too small (the gap for hexagonal holes is 0.52 compared to 0.50 for circular holes) to merit the added complexity of having to etch hexagonal holes. On the other hand, competing objectives like minimization of pressure drop for optofluidic systems [14], isotropy, or local defect optimizations may result in other structures being optimal. Here, our conclusions on the geometric properties of optimal gap structures and their gap values may be of help.

We have also applied our optimization algorithm to the case of full gaps, i.e., simultaneous TM and TE gaps. However, we found no systematism for this case. Future investigations will concentrate on surface plasmons and the full 3D case.

*sigmund@mek.dtu.dk

[1] E. Yablonovitch, Phys. Rev. Lett. **58**, 2059 (1987).
[2] S. John, Phys. Rev. Lett. **58**, 2486 (1987).
[3] E. Lidorikis, M. M. Sigalas, E. N. Economou, and C. M. Soukoulis, Phys. Rev. B **61**, 13458 (2000).
[4] D. Cassagne, C. Jouanin, and D. Bertho, Phys. Rev. B **53**, 7134 (1996).
[5] J. D. Joannopolis, R. D. Meade, and J. N. Winn, *Photonic Crystals: Molding the Flow of Light* (Princeton University Press, Princeton, NJ, 1995).
[6] S. J. Cox and D. C. Dobson, J. Comput. Phys. **158**, 214 (2000).
[7] O. Sigmund and J. S. Jensen, Phil. Trans. R. Soc. A **361**, 1001 (2003).
[8] C. Kao, S. Osher, and E. Yablonovitch, Appl. Phys. B **81**, 235 (2005).
[9] C. Chen, A. Sharkway, S. Shouyuan, and D. Prather, Opt. Express **11**, 317 (2003).
[10] L. Shen, Z. Ye, and S. He, Phys. Rev. B **68**, 035109 (2003).
[11] S. Preble, M. Lipson, and H. Lipson, Appl. Phys. Lett. **86**, 061111 (2005).
[12] Q. Du, V. Faber, and M. Gunzburger, SIAM Rev. **41**, 637 (1999).
[13] M. P. Bendsøe and O. Sigmund, *Topology Optimization—Theory, Methods and Applications* (Springer, New York, 2003).
[14] P. Domachuk, H. Nguyen, B. Eggleton, M. Straub, and M. Gu, Appl. Phys. Lett. **84**, 1838 (2004).